Journal of Structural Geology 33 (2011) 859–874

Contents lists available at ScienceDirect

Journal of Structural Geology

journal homepage: www.elsevier.com/locate/jsg

Paleostress analysis of Cenozoic faulting in the Kraishte area, SW Bulgaria

Alexandre Kounov [a,*], Jean-Pierre Burg [b], Daniel Bernoulli [a,b], Diane Seward [c], Zivko Ivanov [d], Dimo Dimov [d], Ianko Gerdjikov [d]

[a] Institute of Geology and Paleontology, Basel University, CH-4056 Basel, Switzerland
[b] Geological Institute, ETH-Zentrum, CH-8092 Zürich, Switzerland
[c] School of Geography, Environment and Earth Sciences, Victoria University, Wellington, New Zealand
[d] Faculty of Geology and Geography, University "St. Kliment Ohridski", Sofia 1000, Bulgaria

ARTICLE INFO

Article history:
Received 5 June 2010
Received in revised form
4 March 2011
Accepted 8 March 2011
Available online 15 March 2011

Keywords:
Paleostress
Cenozoic extension
Kraishte
SW Bulgaria
Detachment faults
Basin formation

ABSTRACT

Paleostress calculations from fault planes in Paleogene sediments and in the underlying basement were used to determine the orientation and the chronology of the principal stresses during the Cenozoic tectonic evolution of the Kraishte area (southwest Bulgaria). The results show that middle Eocene–early Oligocene WSW–ENE extension led to the formation of grabens and half grabens filled with thick continental to marine deposits in the hanging wall of extensional detachments.

The Paleogene sediments and their basement were then intruded by subvolcanic bodies and dykes during SW–NE extension between 32 and 29 Ma. These WSW–ENE and SW–NE extensional stages are related to the general rollback of the Hellenic slab.

From the late Oligocene to the earliest Miocene, SSE–NNW transtension generated coal-bearing sedimentary basins. The anticlockwise rotation of the main tensile axis by almost 50° with respect to the previous tectonic stage was probably related to a switch from the Aegean back-arc extension to crustal stretching and extrusion of continental fragments around the Moesian platform.

Since the middle Miocene extension in the Kraishte area, accommodated by faults with relatively small displacement, led to the formation of restricted basins filled with alluvial to lacustrine deposits.

1. Introduction

The retreat of the Hellenic subduction is generally regarded as the cause of the formation of the Aegean Sea and the extension in the surrounding regions (e.g. Jolivet et al., 1994; Gautier et al., 1999). Whereas the picture is well established for Oligocene–Miocene times and after, some uncertainty remains concerning the localization and the extension directions during the earlier evolution of the Hellenides back-arc region. An additional question concerns the transition from previously compressional to extensional tectonics. By and large, the Cenozoic tectonic evolution of the northern Aegean region (Serbia, Macedonia, southern Bulgaria, northern Greece and Turkey) was accompanied by magmatism and basin formation (e.g. Jolivet et al., 1994; Burchfiel et al., 2000). Extension probably started in the middle to late Eocene and migrated southwards in the Aegean Sea region (Burchfiel et al., 2000; Kounov et al., 2004). Initially NE–SW to NNE–SSW oriented, it changed to almost N–S at the beginning of the Pliocene (~6 Ma, Gautier et al., 1999; Burchfiel et al., 2000, 2003, 2008; Nakov et al., 2001; Dumurdzanov et al., 2005). A short-lived period of shortening during the late Oligocene to early Miocene was reported from Macedonia and south Bulgaria (Burchfiel et al., 2000, 2003, 2008; Nakov et al., 2001; Dumurdzanov et al., 2005); however, this seems to be regionally restricted and was possibly associated with local transpression on restraining fault segments.

In this ongoing discussion, Cenozoic extension in the Kraishte zone of Southwestern Bulgaria (Fig. 1) has been documented essentially through the evolution of sedimentary basins during this time (Fig. 2, e.g. Kamenov, 1942; Belmoustakov, 1948; Moskovski and Shopov, 1965; Moskovski, 1968b, 1969, 1971a, 1971b; Zagorchev and Popov, 1968; Moskovski and Harkovska, 1973; Harkovska, 1974; Zagorchev et al., 1989). Sedimentation in these basins had probably already started during the middle Eocene and intermittently continued to the present (Moskovski and Shopov, 1965; Harkovska, 1974; Zagorchev et al., 1989; Bakalov and Jelev, 1996; Kounov, 2002). The successive formation and inversion of the Cenozoic basins was attributed to several extensional and compressional tectonic phases (Moskovski, 1968a, 1969, 1971a; Moskovski and Harkovska, 1973; Burchfiel et al., 2000). Moskovski and Harkovska (1973) have reported at least four

* Corresponding author. Fax: +41 612673613.
E-mail address: a.kounov@unibas.ch (A. Kounov).

0191-8141/$ – see front matter © 2011 Elsevier Ltd. All rights reserved.
doi:10.1016/j.jsg.2011.03.006

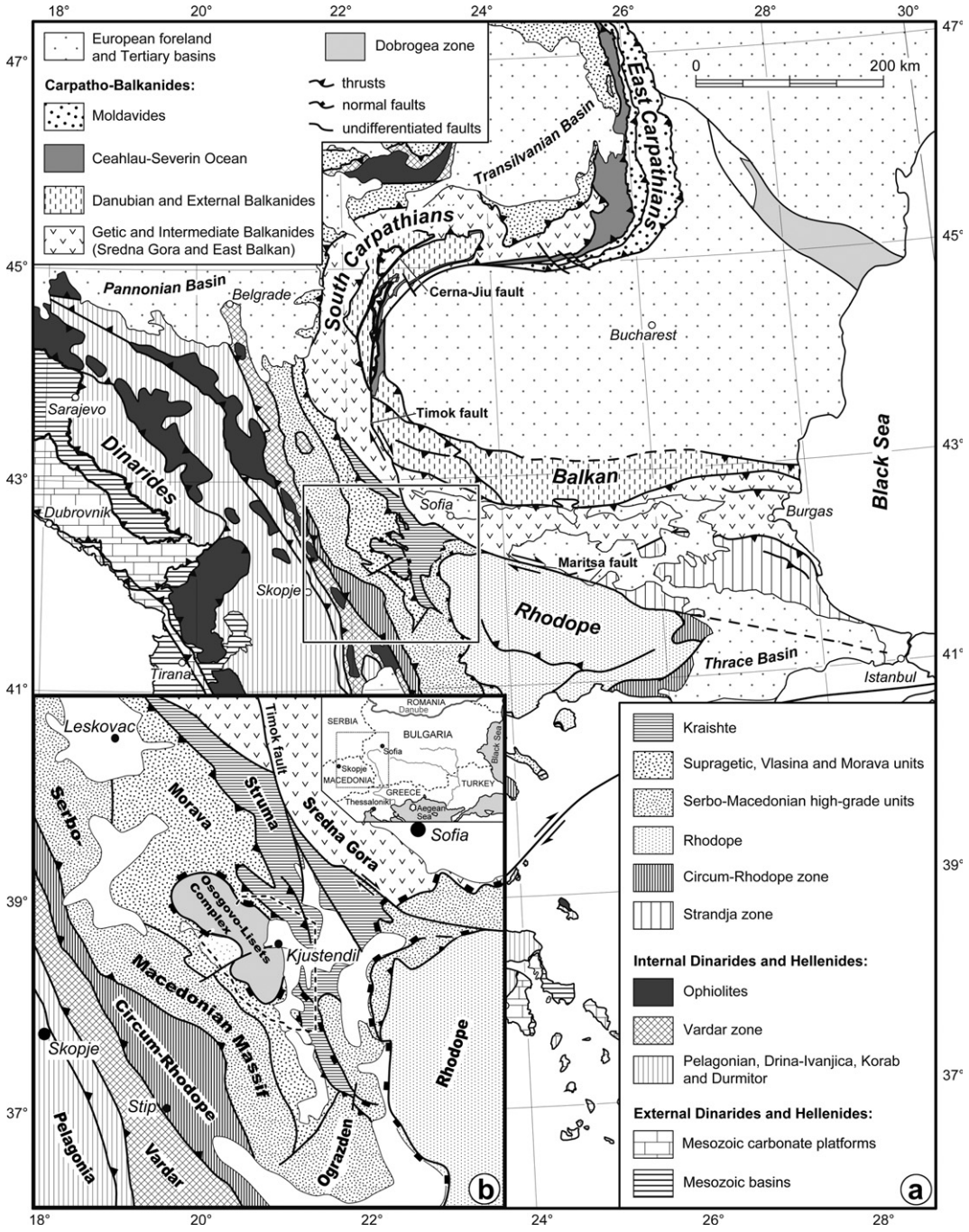

Fig. 1. a) Tectonic map of the southwestern Balkan Peninsula (after Schmid et al., 2008). Box outlines Fig. 1b. b) Tectonic overview of the Kraishte area (dashed line for studied area).

Paleogene and two Neogene tectonic phases related to the successive alternation of generally NE–SW oriented extension and compression; however, these authors did not attempt to correlate the Cenozoic tectonic evolution in Kraishte to that of the rest of the Balkan Peninsula.

Until now the orientation of the tectonic forces during the Cenozoic in the Kraishte area was approximated only on the basis of fault orientations and relative movements along them, without detailed structural and paleostress studies. Comprehensive structural studies combined with thermochronological data have shown that the early stages of Cenozoic extension resulted in the formation of an extensional core complex exhumed along low-angle detachment faults (Graf, 2001; Kounov et al., 2004).

In this study, we carried out paleostress calculations from fault data within the Paleogene sediments and their underlying basement in order to constrain the chronology and the orientation of the paleostress fields during the Cenozoic tectonic evolution of the area. Considering that the major fault structures are very poorly exposed, we have analyzed mainly meso-fractures, which are reliable indicators of the regionally significant stress/strain trajectories. Our results revealed the existence, in the Cenozoic, of at least three consecutive extensional phases in the Kraishte area. The middle Eocene–early Oligocene extension was WSW–ENE and led to the formation of the Osogovo-Lisets extensional core complex (Kounov et al., 2004). It was followed, in the early Oligocene by a SW–NE-oriented, syn-magmatic extensional phase. The extension

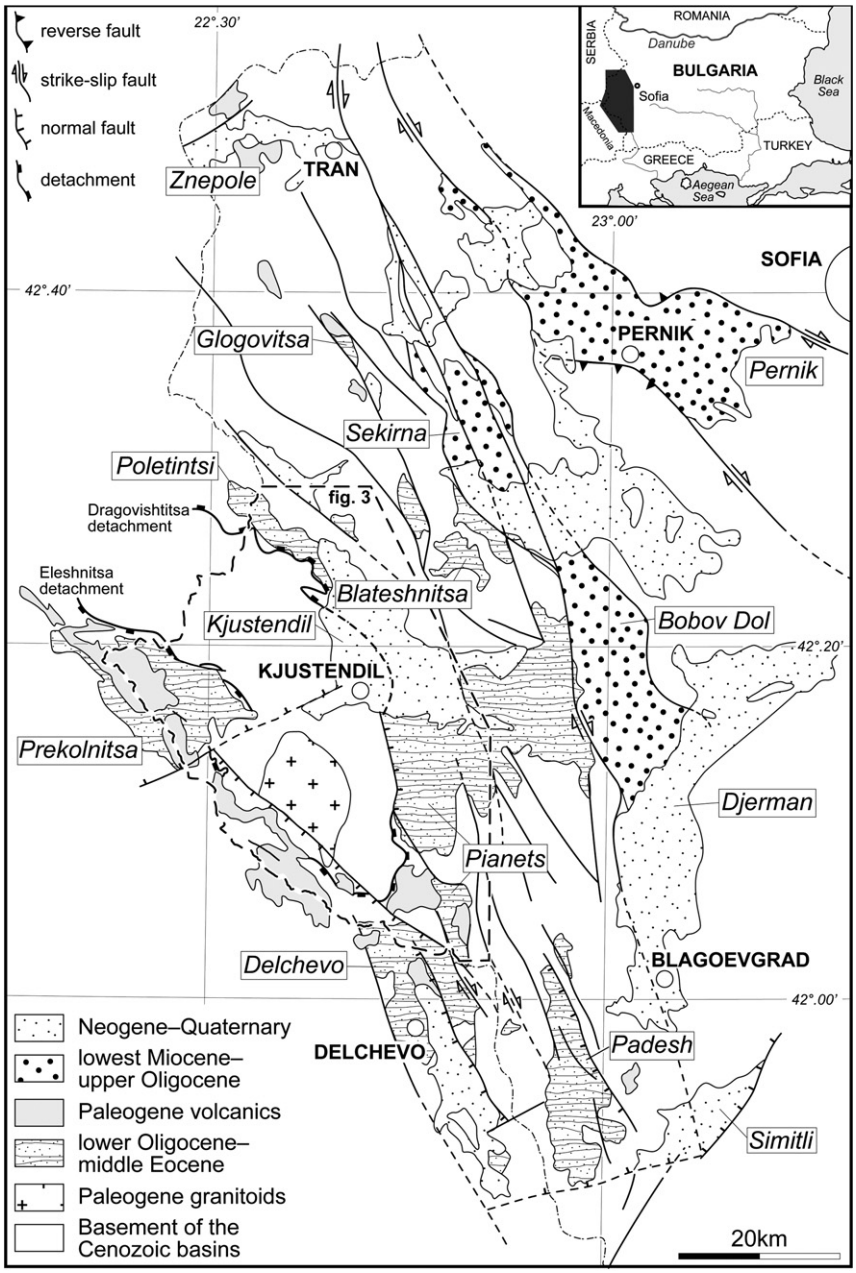

Fig. 2. Map of the Paleogene and Neogene basins and major fault structures in the Kraishte zone, adapted from Zagorchev et al. (1989).

direction rotated toward NNW–SSE and was related to transtension and formation of continental basins since the late Oligocene.

2. Geological setting

The Kraishte region, in western Bulgaria, is located between the Serbo-Macedonian high-grade metamorphic unit to the SW, the Rhodope "Massif" to the SE and the European margin (late Cretaceous Sredna Gora volcanic arc) to the N (Fig. 1). During the late Early Cretaceous, the greenschist metamorphic basement and its early Paleozoic sedimentary cover of the Morava unit was thrust onto the Struma unit, composed of a basement of variably deformed continent- and ocean-derived magmatic rocks of Vendian age (570–540 Ma, Graf, 2001; Kounov, 2002), covered by Permian to Lower Cretaceous sediments (Fig. 1, e.g. Dimitrov, 1931; Bonchev, 1936; Zagorchev and Ruseva, 1982; Graf, 2001; Kounov et al., 2010). During the Cenozoic, the Osogovo-Lisets metamorphic complex was exhumed from below the Struma unit along the Dragovishtitsa and Eleshnitsa detachment faults (Figs. 2 and 3). Extension started in the middle Eocene and generated sedimentary basins where syn-tectonic continental and brackish clastic sediments were deposited (Fig. 3, Kamenov, 1942; Belmoustakov, 1948; Moskovski and Shopov, 1965; Zagorchev et al., 1989; Zagorchev, 2001; Kounov, 2002). In the late Eocene, the detachments became inactive and were sealed by marine, volcano-sedimentary series, the deposition of which continued in the early Oligocene (Belmoustakov, 1948; Kounov, 2002). The Middle Eocene–Lower Oligocene sediments and their basement were intruded by rhyolitic to dacitic subvolcanic bodies and dykes; K/Ar radiometric ages on feldspar phenocrysts and whole rock samples scatter from 30 ± 1 to 32 ± 1 Ma (Harkovska and Pecskay, 1997) and the zircon fission-

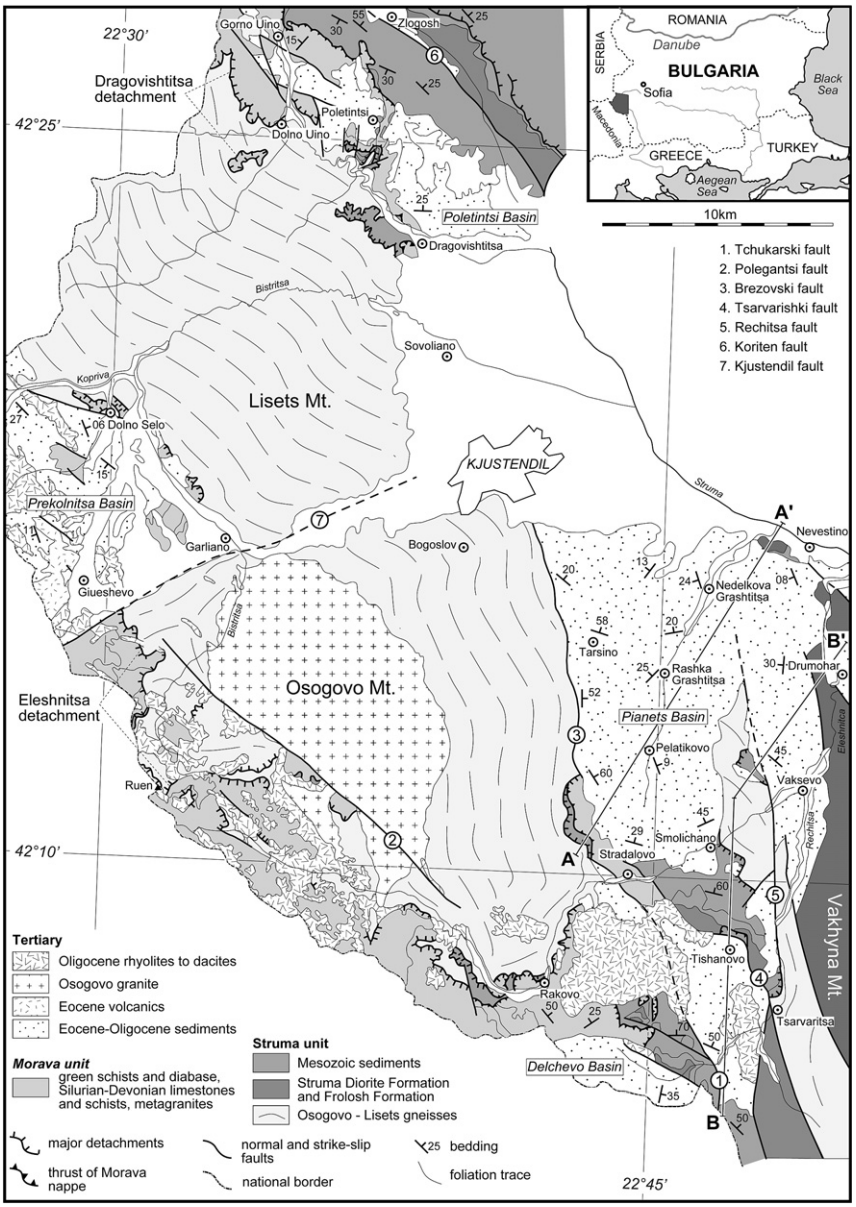

Fig. 3. Geological map of the part of Kraishte area (SW Bulgaria) modified from Moskovski (1968b), Zagorchev (1993) and Zagorchev and Ruseva (1993). Line AA′ and BB′ are the sections in Fig. 5.

track ages are as young as 29 Ma (Kounov et al., 2004). During the middle Eocene and early Oligocene, sedimentation was restricted to local depocentres: the Padesh, Poletintsi and Pianets basins to the south; the Prekolnitsa, Blateshnitsa and Glogovitsa basins to the north (Figs. 2 and 3).

From late Oligocene to early Miocene, terrigenous coal-bearing sediments were unconformably deposited in continental basins (Fig. 2, Bobov Dol, Sekirna and Piernik basins). Deposition of alluvial to lacustrine material in the Neogene–Quaternary basins represents the last stage of sedimentation (Fig. 2, i.e. Kjustendil and Djerman basins).

Previous authors (e.g. Bonchev et al., 1960; Moskovski, 1969, 1971a; Bonchev, 1971; Moskovski and Harkovska, 1973) have described two main sets of Cenozoic faults in the Kraishte zone. One set, striking NW–SE, includes the Polegantsi and Koriten faults (Fig. 3), whereas the other, including the Brezovski, Rechitsa and some other faults, strikes NNW–SSE. Previous authors proposed that most of the NNW–SSE and some NW–SE faults acted as normal faults during the early SW–NE, late Eocene–early Oligocene extension. The second tectonic stage was interpreted as SW–NE compression and reactivation of pre-existing faults (such as Brezovski, Tsarvarishki and Rechitsa faults on Fig. 3) as strike-slip and reverse faults, leading to basin inversion and the end of sedimentation (Moskovski, 1969; Moskovski and Harkovska, 1973); however, we could not recognize this stage as a regional event by our data. The third stage was related to Oligocene SW–NE extension and the emplacement of the shallow rhyolitic to dacitic intrusions and dykes, mainly along the NW–SE fault zones (Fig. 3). Neogene tectonics of the area was thought to be related to strike-slip and normal faults, such as the Kjustendil fault, and the formation of the Kjustendil basin (Figs. 2 and 3, Moskovski, 1969; Moskovski and Harkovska, 1973).

3. Methodology

3.1. Stress inversion from fault-slip data

Fault planes and associated striations with kinematic indicators were measured at eleven sites within Paleogene sediments and their basement, to determine paleostress directions of pre- and post-sedimentary deformation (Fig. 4). The collection of a fault-slip datum includes fault plane orientation, slip direction, and the sense of slip (reverse, normal, dextral, or sinistral). All of the analyzed faults are discrete fractures without gouge and breccia zones. Most of the observed fault planes, especially in the Cenozoic sediments, bear only striated slip planes without new crystallization. The faults with slicken fibers (calcite, chlorite, epidote) were observed mostly in the Triassic limestones and some of the metamorphic basement rocks. Therefore the faulting style and type of the mineral coating were not used to help the characterization of homogenous fault populations. Conjugate fault sets were used in the field for an on-site, first estimate of the bulk shortening/stretching directions. Senses of fault slip were determined using standard sense-of-slip criteria (e.g. Hancock, 1985; Petit, 1987). Assuming that the direction and sense of motion on a variety of fault planes in a rock mass are derived from one "stress" tensor that affected the area during a certain period, one may subdivide a heterogeneous set of fault-slip data into homogeneous fault subsets. Heterogeneities and anisotropies in the rock mass are sources of variation in tensor orientation and ratio. Most of such disturbances have little influence but still can locally play an important role. Therefore, to strengthen the validity of local determinations, the obtained local paleostress tensors have to be consistent on a regional scale. The homogeneous fault subsets could be best identified directly in the field by observation of cross-cutting relations between individual faults or by superimposition of striae on the same fault plane. When such information is missing or scarce, additional separation

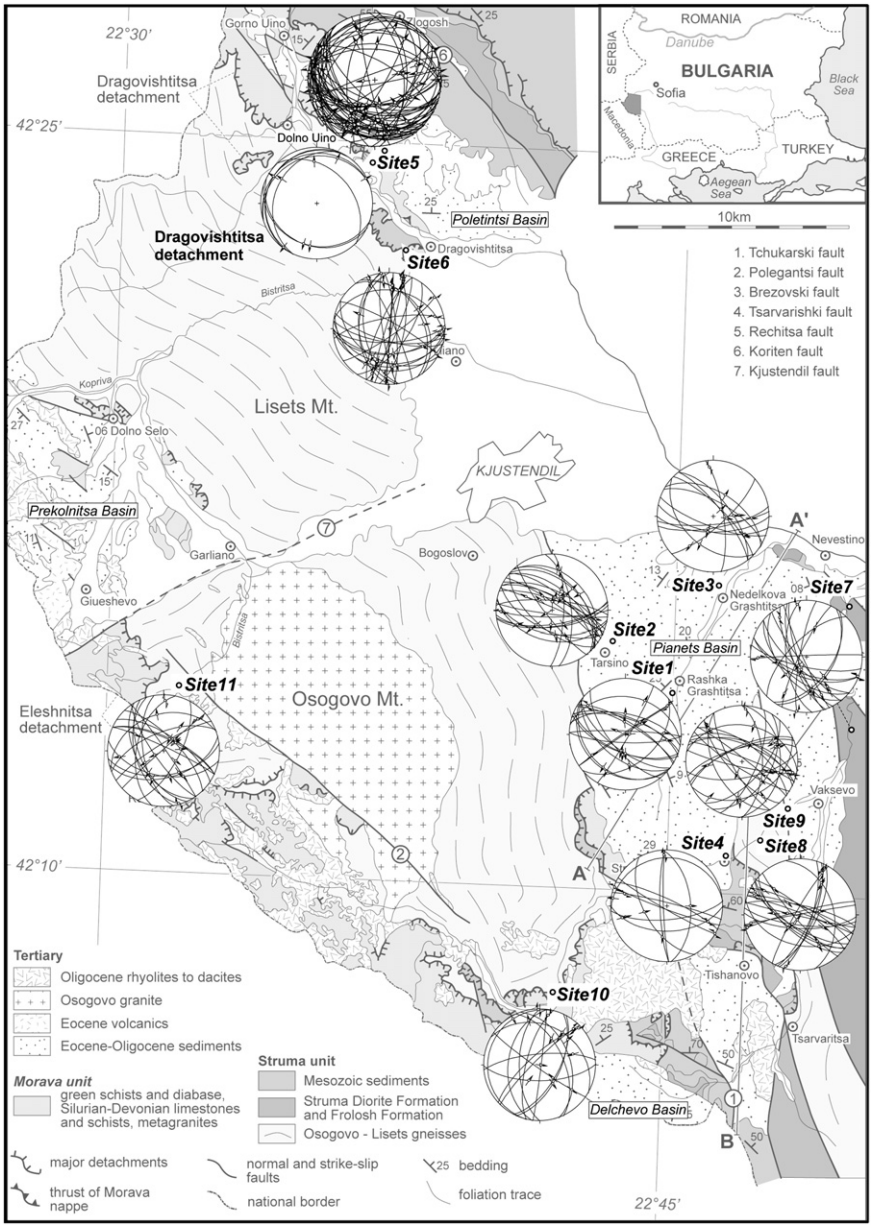

Fig. 4. Unseparated fault data from 11 sites. Fault/striation plotted in stereonet, lower hemisphere (fault planes: great circle, striation: arrow, pointing toward movement of the hanging block).

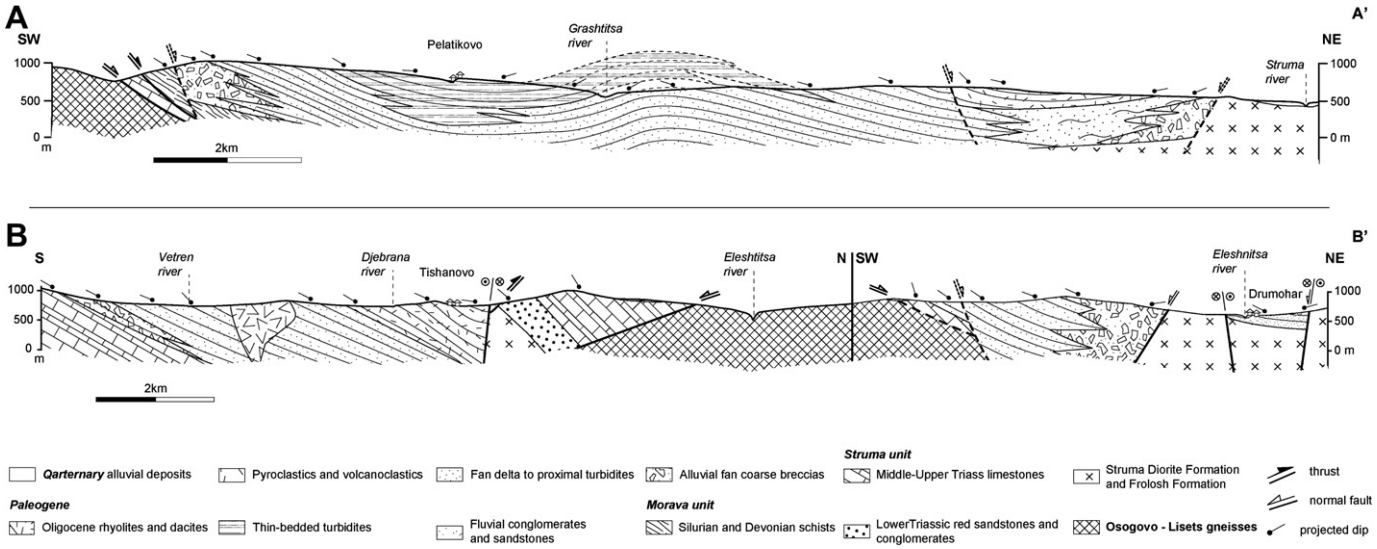

Fig. 5. Cross-sections through the Pianets basin. For location see Fig. 3 trace AA′ and BB′.

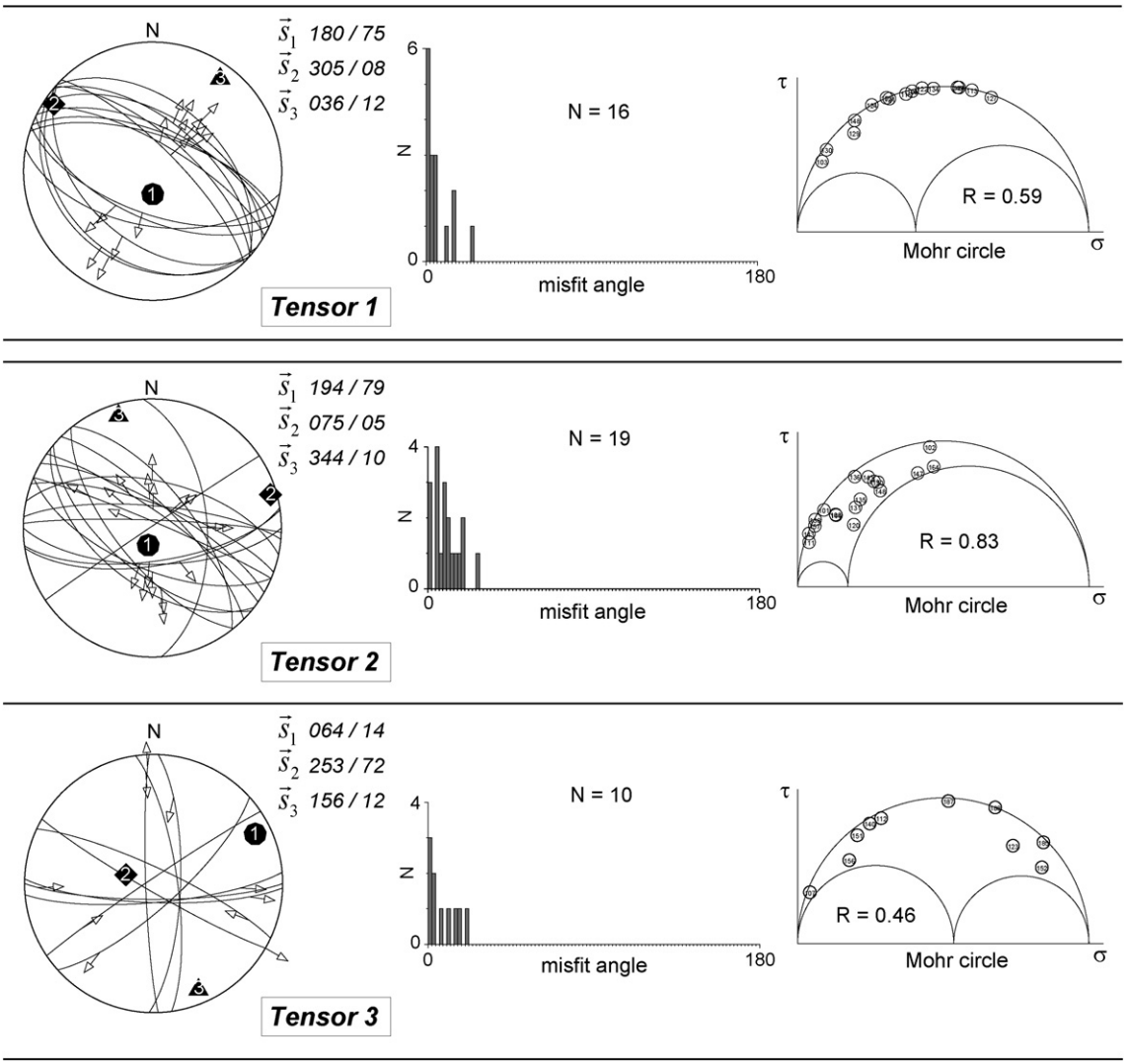

Fig. 6. Lower hemisphere, equal-area plots of brittle fault-slip striations from the Pianets basin. Orientations of the stress axes are plotted (circle – $\sigma 1$ compressional axis, square – $\sigma 2$ intermediate axis, triangle – $\sigma 3$ tensional axis). Distribution of the misfit angle is given in the histogram (N: number of faults, x-axis: misfit angle) and the stress tensor aspect ratio R is represented in a Mohr circle diagram (τ: shear stress, σ: normal stress).

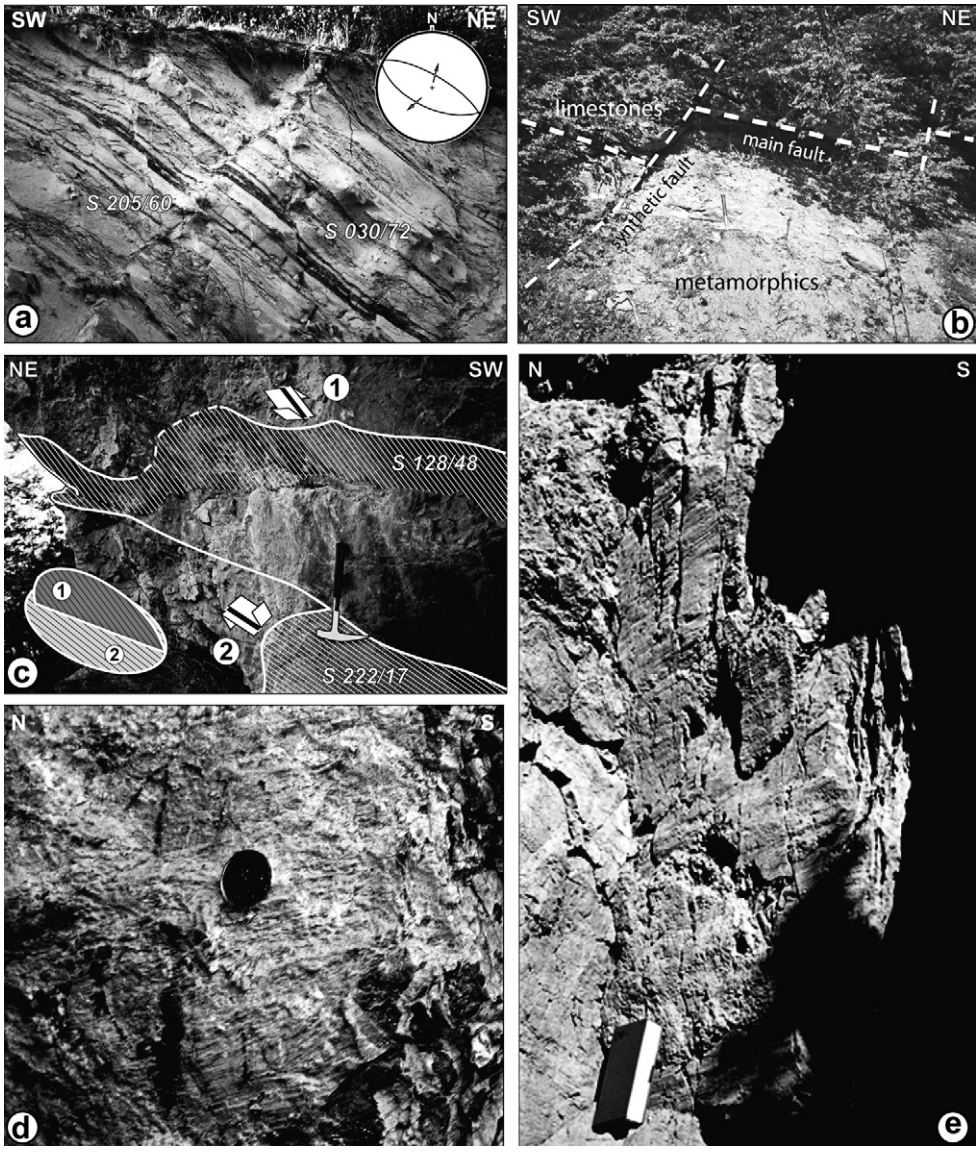

Fig. 7. a) Conjugate normal faults in the Paleogene sediments near Tarsino. b) Eleshnitsa detachment near Vaksevo. The main fault is cut by synthetic faults. c) Brittle faults in the Triassic limestones near Poletintsi. A SW-dipping normal fault (2) cuts the SE-dipping reverse fault (1). d) Riedel shears showing a dextral sense of shear in the Triassic limestones near Dragovishtitsa. e) Oblique stylolites showing a dextral sense of shear in the Triassic limestones near Dragovishtitsa.

techniques must be applied. Several different approaches, especially developed for the separation of the different stress tensors from heterogeneous fault-slip data, have been usefully used recently (e.g. Sperner et al., 1993; Célérier, 1999; Yamaji, 2000; Sippel et al., 2009; Viola et al., 2009; Heuberger et al., 2010).

In this study the data processing was carried out using the Fault Slip Analysis (FSA) software (Célérier, 1999) based on a direct inversion algorithm, which assumes that the shear stress applied to each fault plane is parallel to the observed slickenline (Bott, 1959; Compton, 1966; Angelier, 1979; Etchecopar et al., 1981; Angelier et al., 1982). The program uses the Monte Carlo inversion procedure, similar to that developed by Etchecopar et al. (1981), to search for stress tensors that yield shear stress directions as close as possible to the measured slip directions of the given dataset. The principal stress directions $\vec{s}_1$, $\vec{s}_2$ and $\vec{s}_3$, and the stress tensor aspect ratio, $R=(\sigma_1-\sigma_2)/(\sigma_1-\sigma_3)$, where σ_1, σ_2 and σ_3 (the greatest, intermediate and least compressive stresses) are the principal stress magnitudes corresponding to $\vec{s}_1$, $\vec{s}_2$ and $\vec{s}_3$ (eigenvectors) respectively, were determined. The misfit angle, representing the angle between the calculated maximum shear stress and the measured slip direction for each individual fault plane was also calculated. The stress ratio describes the shape of the ellipsoid for homogeneous fault subsets (Appendix 1, Célérier, 1988, 1995). An R-value close to 1 indicates small differences between σ_1 and σ_3, whereas R is close to 0 when σ_1 and σ_2 are almost equal. Here we use the stress tensor aspect ratio defined in Célérier (1988) ($R=(\sigma_1-\sigma_2)/(\sigma_1-\sigma_3)$) as it is presenting more directly the differential stress than the stress ratio $R=(\sigma_2-\sigma_3)/(\sigma_1-\sigma_3)$ used by Angelier (1979). Methods based on this approach construct kinematic (or strain) axes for each individual fault plane assuming that, under upper crustal deformation conditions, the axes of strain coincide with the axes of stress (e.g. Anderson, 1951). This technique makes no assumption concerning the attitude of fault planes relative to stress axes. As a result, whether a fault plane is newly created or results from reactivation of an older discontinuity does not affect the reconstruction of the paleostress tensor. This is important because many fault movements have occurred along older faults, joints, bedding planes and other discontinuities of weakness.

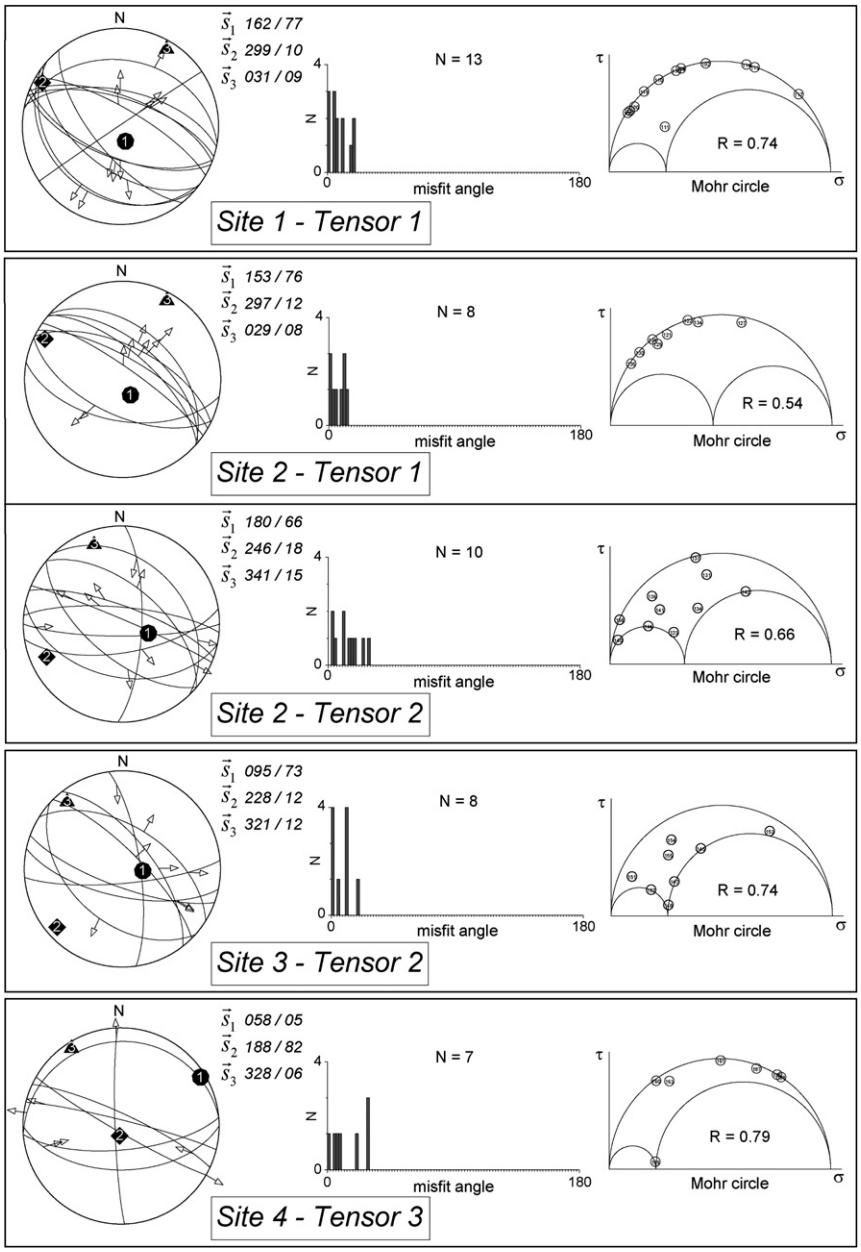

Fig. 8. Lower hemisphere, equal-area plots of brittle fault-slip striations from the Pianets basin sediments. Localities of the sites are shown on Fig. 4. Legend as in Fig. 6.

3.2. Paleostress tensor calculation

The different paleostress tensors were calculated following the general logic of paleostress reconstructions where successive tectonic events are filtered by starting from the youngest rock, which contains only the last tectonic record, toward the oldest rocks, which record an increasing number of events. This is of course only possible if the successive tectonic events do not have similarly oriented stress axes in which case two events of different age could be erroneously interpreted as one single young event. In our study the obtained stress tensors attributed to different tectonic events differ significantly, which gives some confidence in the results.

To determine the bulk brittle tectonics in the Cenozoic sediments and eliminate local deviations, all measurements were processed as one dataset. In the first step, the 20 tensors best fitting 30% of the measurements were randomly calculated. This random search is a Monte Carlo approach to extract a stress tensor that best explains the slip directions. The 20 tensors obtained from this first calculation already revealed three groups of similarly oriented principal stress axes, which suggested that the dataset includes at least three phases of fault movements. From these 20 tensors, the tensor that integrated the highest number of small misfit angles $\alpha < 30^\circ$ was chosen for further calculation to obtain the best fit for 70% of the data. Once separating the fault data related to the obtained stress tensor from the dataset, the same procedure was applied to the remaining measurements. After several iterations, three stress tensors that embrace most of measured faults were finally recognized.

In a second step, the three calculated stress tensors were imposed on all measurements from each site in the study area. This is the process where the program searches the faults that fit the regional stress tensors at each site. In this way, the data that fit the regional tensors underwent independent random tensor searches to check their interpretation and to sort out local deviations. We rearranged the subsets by comparing faults best fitting the tensors

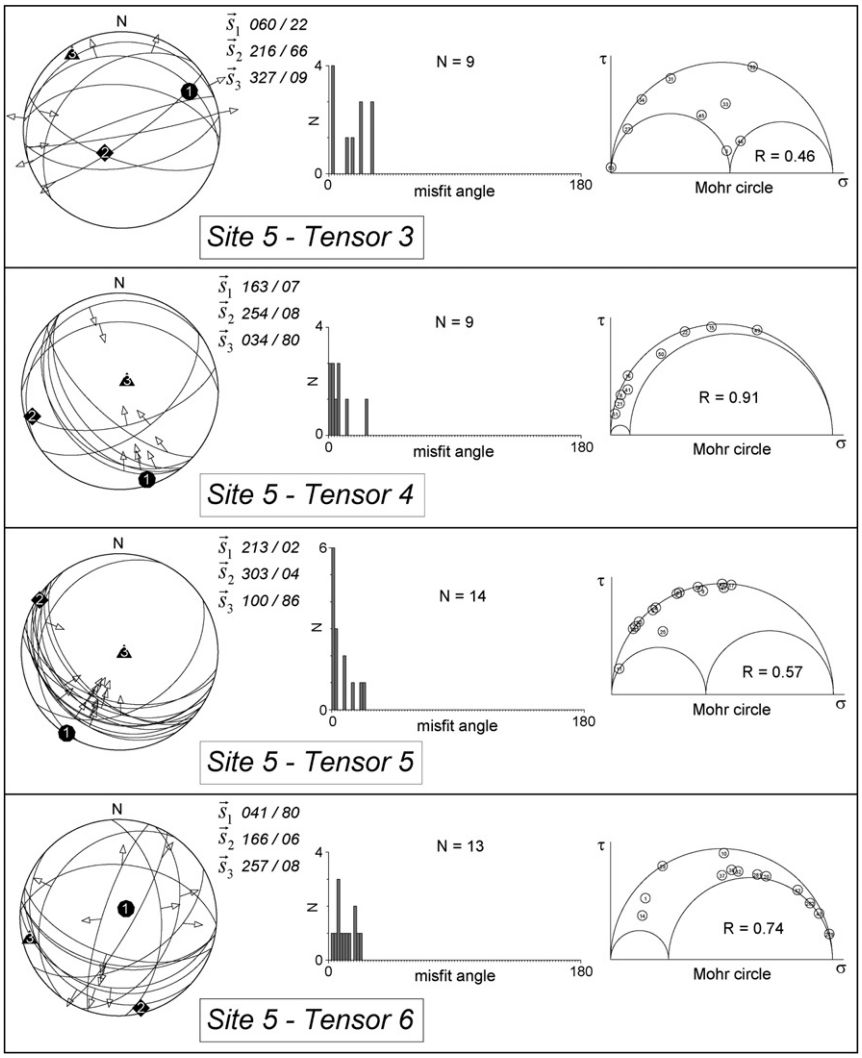

Fig. 9. Lower hemisphere, equal-area plots of brittle fault-slip striations from the Triassic limestones above the Eleshnitsa detachment north of Poletintsi (*Site 5*, Fig. 4). Legend as in Fig. 6.

obtained through single site separation with the fault population obtained by imposing the regional tensors. Further rearrangements in the data subsets were sometimes performed and compared to populations identified from geological observations.

The calculated tensors were not all obtained at every site. Some tensors may have escaped calculation either because the relevant fault population was locally too small, or because the site area did not deform during a particular brittle event. Regional correlation from site to site relies on both the orientation and the shape of stress tensors and the chronological sequence based on field relationships between identical fault and striation sets.

4. Data processing and results

4.1. Paleostress tensor analysis in the Paleogene sediments

Structural investigations were carried out in the Middle Eocene–Lower Oligocene sediments of the Pianets basin in more detail than elsewhere (Fig. 4).

Deformation of the basin sediments is weak. Beds are tilted and folded into large-scale (>1 km wavelength) gentle folds (Fig. 5). Apart from soft-sediment slump folds, meso-scale folds have not been observed. Tilting of the basement blocks as well as depositional

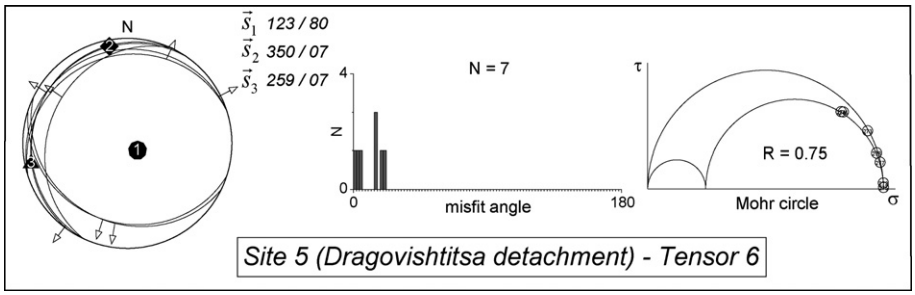

Fig. 10. Lower hemisphere, equal-area plots of brittle fault-slip striations measured on the fault plane of the Dragovishtitsa detachment north of Poletintsi (*Site 5*, Fig. 4). Legend as in Fig. 6.

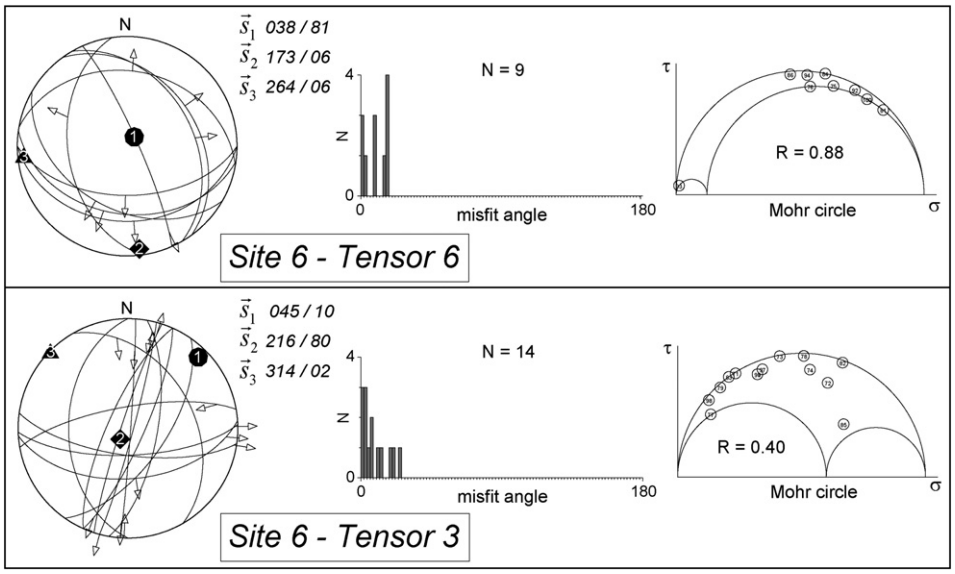

Fig. 11. Lower hemisphere, equal-area plots of brittle fault-slip striations from the Triassic limestones above the Eleshnitsa detachment near Dragovishtitsa (*Site 6*, Fig. 4). Legend as in Fig. 6.

geometries such as sedimentary wedges along the basin margins suggest that the basin evolution was controlled by listric normal faults (Fig. 5), with which large-wavelength folds may be associated.

Fault planes and striations were measured at four locations in the sedimentary series (*Sites 1* to *4*, Fig. 4). Following the procedure presented in the Methodology paragraph, three regional stress tensors were obtained from the bulk fault dataset. The first tensor integrates NW–SE trending conjugate normal faults (Figs. 6 and 7a). The sub-horizontal tensile axis ($\vec{s}_3$) is SW–NE (036/12°). Despite the fact that the stress tensor was obtained from conjugate fault sets, the calculated *R*-value of 0.59 does not show axial extension (Appendix 1) probably due to the relative spread of the striation orientations (Fig. 6). The second tensor is obtained from NW–SE to W–E normal and strike-slip faults. The horizontal tensile axis ($\vec{s}_3$) is NNW–SSE (344/10°) and the compressive axis ($\vec{s}_1$) is vertical (Fig. 6). The high *R*-value (=0.83) indicates nearly radial extension (Appendix 1). The third tensor mostly stems from strike-slip faults. The calculated main compressional $\vec{s}_1$ (064/14°) and tensile $\vec{s}_3$ axes (156/12°) are horizontal (Fig. 6). The sub-vertical intermediate axis $\vec{s}_2$ and $R = 0.46$ suggest a strike-slip regime (Appendix 1).

In *Site 1* (Fig. 4), the estimated $\vec{s}_3$ is horizontal and SW–NE-oriented like the regional *Tensor 1* (*Site 1*, Fig. 8). High *R*-values indicate radial extension. In *Site 2*, two tensors fit the *Tensor 1* and *Tensor 2* (*Site 2*, Fig. 8). The first tensor is derived from NW–SE normal faults, whereas the second one mostly integrates strike-slip faults. The tensor calculated for *Site 3* corresponds to *Tensor 2* (*Site 3*, Fig. 8).

Near Smolichano (*Site 4*, Fig. 4) several conjugate strike-slip faults were measured. Kinematic indicators are mostly slicken fibers. The intermediate axis $\vec{s}_2$ is sub-vertical and the stress ratio $R = 0.79$. The tensile axis $\vec{s}_3$ is NNW–SSE (328/06°) like that of the regional *Tensor 3*.

4.2. Paleostress tensor analysis in the basement of the Paleogene sediments

Fault planes and striations at seven locations in the Struma unit and the Osogovo-Lisets Complex were also treated for paleostress calculations (Fig. 4).

The stress tensors obtained from the Middle Eocene–Lower Oligocene sediments must be related to post-early Oligocene tectonics. Therefore, basement data that would fit these tensors were first sought. Data that did not fit the previously defined three tensors underwent the same procedure as data from the sedimentary basins in order to determine possibly older stress tensors. The data that fit the tensors from the sediments also underwent another random tensor search to check their reliability and to sort out local deviations.

South of the village of Poletintsi, in the Poletintsi river valley (*Site 5*, Fig. 4), 57 fault planes and striations were measured in Triassic limestones. Most of the fault data did not fit any of the stress tensors obtained from the Paleogene sediment. The only exception is the small population of 9 strike-slip and normal faults giving a poorly

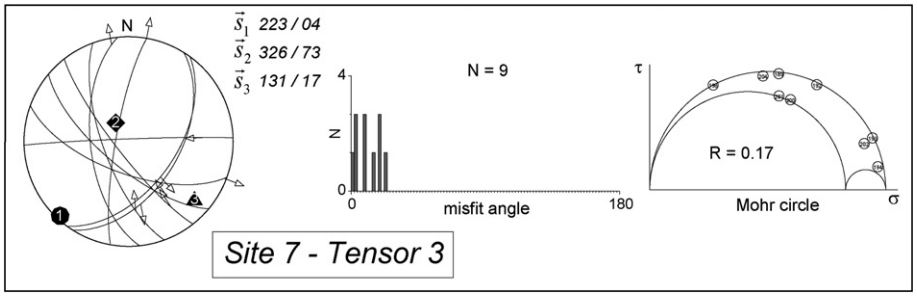

Fig. 12. Lower hemisphere, equal-area plots of brittle fault-slip striations from the Struma unit along the Eleshnitsa river (*Site 7*). Localities of the sites are shown on Fig. 4. Legend as in Fig. 6.

constrained tensor similar to the *Tensor 3* (Fig. 9). The obtained tensile NW–SE oriented $\vec{s}_3$ axis is horizontal and NW–SE oriented.

From the rest of the fault data three tensors were obtained (Fig. 9). *Tensor 4* integrates dominantly SW- to SE-dipping thrust faults. The compression $\vec{s}_1$ axis is horizontal and trends SSE–NNW. The stress ratio $R = 0.91$ suggests axial compression.

Tensor 5 stems from mostly SW-dipping thrust faults with SW-plunging striations (Fig. 9). The compressive $\vec{s}_1$ axis is sub-horizontal and SSW–NNE oriented. The tensile stress axis $\vec{s}_3$ is sub-vertical and the *R*-ratio = 0.57.

Tensor 6 was obtained mostly from SW-dipping normal faults. The WSW–ENE tensile $\vec{s}_3$ axis is sub-horizontal (Fig. 9). The stress ratio $R = 0.74$ suggests radial extension. This stress tensor is similar to that obtained from fault measurements on the fault plane of the Dragovishtitsa detachment from the same site (Fig. 10).

Near Dragovishtitsa, 31 strike-slip and normal faults were measured in the Triassic limestones above the Dragovishtitsa detachment (*Site 6*, Fig. 4). Two tensors were obtained. The first characterized by a vertical $\vec{s}_1$ axis and the second by a vertical intermediate $\vec{s}_2$ (Fig. 11). The first tensor is obtained from W–E and NNW–SSE-striking normal faults and has a tensile axis $\vec{s}_3$ trending E–W like the tensile axis obtained from the detachment plane in the Poletintsi area (Fig. 10). This tensor is similar to *Tensor 6* from *Site 5* (Fig. 9) and is therefore probably related to the same tectonic event. The second tensor integrates mostly W–E and SSW–NNE strike-slip faults (Fig. 7d and e). The tensile axis $\vec{s}_3$ trends NW–SE, like the regional *Tensor 3* (Fig. 11).

Fault planes and striations were measured along the Eleshnitsa River, near Drumohar, in magmatic rocks of the Struma unit (*Site 7*, Fig. 4). The calculated principal compressional $\vec{s}_1$ (223/04°) and tensile $\vec{s}_3$ axes (131/17°) are both horizontal (*Site 5*, Fig. 12). The sub-vertical intermediate stress axis $\vec{s}_2$ and the *R*-ratio = 0.17 suggest transtension (Appendix 1). The SE–NW orientation of the tensile axis $\vec{s}_3$, as *Tensor 3* from the sediments, indicates that these faults are likely related to the same faulting event.

Two tensors were obtained from 22 fault data in the Osogovo-Lisets metamorphic rocks, along the Eleshnitsa River between Smolichano and Vaksevo, (*Site 8*, Fig. 4). They correspond to regional *Tensor 1* and *Tensor 2* (*Site 8*, Fig. 13). The small difference to tensor orientations obtained in the sediments may denote late rotation during strike-slip faulting or deviations controlled by pre-existing faults in the basement.

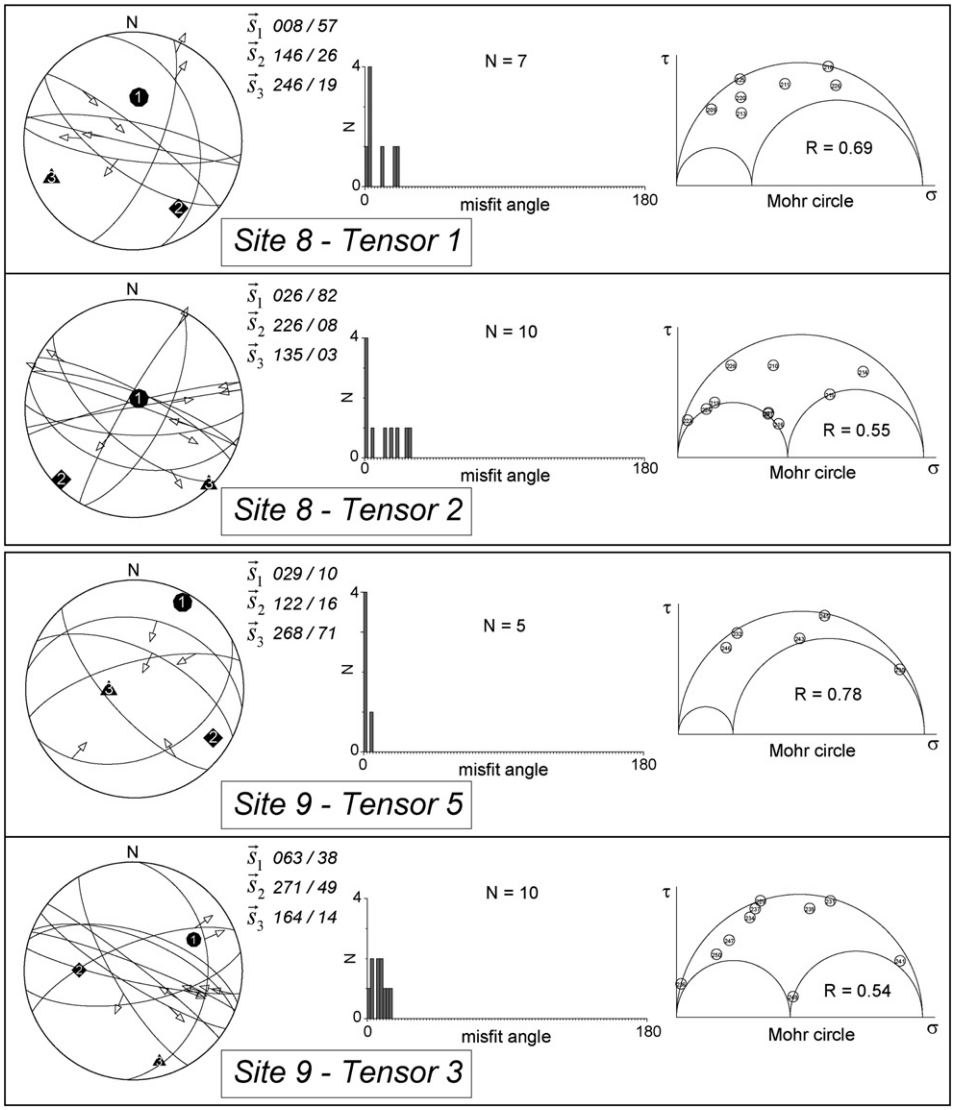

Fig. 13. Lower hemisphere, equal-area plots of brittle fault-slip striations from the Osogovo-Lisets metamorphics and Triassic limestones between Smolichano and Vaksevo. Localities of the sites are shown on Fig. 4. Legend as in Fig. 6.

The paleostress calculation on faults in Triassic limestones near Vaksevo (*Site 9*, Fig. 4) gives two tensors. The first tensor is poorly constrained by 5 reverse faults. The compressional axis ($\vec{s}_1$) is SW–NE (*Site 9*, Fig. 13). This tensor has an orientation similar to that of the *Tensor 4* from *Site 5* (Fig. 9). The second tensor mostly integrates strike-slip faults. The sub-vertical intermediate axis $\vec{s}_2$ (271/49°) and the *R*-ratio = 0.54 suggest pure strike-slip conditions (*Site 9*, Fig. 13). The inclination of the $\vec{s}_2$ axis is possibly related to later block tilting. The SE–NW orientation of the tensile axis $\vec{s}_3$ is close to that of *Tensor 3* from the Paleogene sediments.

In the area of Rakovo, in the Triassic limestones above the Eleshnitsa detachment (*Site 10*, Fig. 4), paleostress calculation was carried out on 7 normal and strike-slip faults. These faults cut the brittle detachment plane (Fig. 7b). The calculated main tensile $\vec{s}_3$ axis (160/25°) is sub-horizontal and $\vec{s}_1$ is sub-vertical (*Site 10*, Fig. 14). This tensor is similar to the regional *Tensor 2* (Fig. 9).

In the Bistritsa valley, the Osogovo-Lisets metamorphics and the intruded Oligocene rhyolitic dykes show the same set of brittle faults (*Site 11*, Fig. 4). The paleostress calculation on 11 faults yielded a sub-horizontal, SW–NE tensile axis ($\vec{s}_3$) (*Site 11*, Fig. 14). The stress ratio $R = 0.92$ suggests radial extension. This stress tensor is similar to *Tensor 1* and is probably related to the movement along the Polegantsi fault (Fig. 4), which belongs to the NW–SE fault set. These faults are younger than the detachment and may have been serving as conduits for the late rhyolitic magma pulses intruded along the southwestern slope of the Osogovo Mountain (Figs. 2 and 3, Moskovski, 1971a; Vardev, 1987).

5. Discussion

Most of the presently exposed pre-Cenozoic basement rocks in the Kraishte area, except the Osogovo-Lisets metamorphic complex, have recorded a relatively long period of brittle deformation, starting probably already in the Paleozoic (Zagorchev and Ruseva, 1982; Kounov et al., 2010). Therefore, in order to define the different tectonic episodes and their relative chronology, it was necessary to analyze faults in rocks of different ages. Defining the pre-Cenozoic stress tensors from heterogeneous fault-slip data in the basement rocks was only possible when tensors corresponding to those obtained from the Paleogene sediments were first determined and related faults extracted from the whole dataset.

Here we discuss tectonic events from the youngest to the oldest to follow the general logic of paleostress reconstructions where successive tectonic events are filtered by starting from the youngest rock that contains the youngest tectonic record, toward the oldest rocks, which record an increasing number of events.

Field relationships show that, in general, strike-slip faults cut normal faults in the Paleogene sediments. Accordingly, it is assumed that *Tensor 1* is related to the earliest phase of deformation (**D3**, Fig. 15) in the sediments. This SW–NE extension may have generated the NW–SE faults, such as Polegantsi fault at *Site 11* (Fig. 4). *Tensor 2* indicates that the extension direction rotated toward NNW–SSE around the sub-vertical $\vec{s}_1$. Many normal faults related to this tensor have the same orientation as the earlier faults but related striations are N–S. These fault planes were obviously reactivated under the second tensor. *Tensor 3* has its tensile axis ($\vec{s}_3$) similar to that of *Tensor 2*. Swapping $\vec{s}_1$ and $\vec{s}_2$ likely reflects local effects and depends whether normal faults ($\vec{s}_1$ vertical) or strike-slip faults ($\vec{s}_2$ vertical) are more abundant. Therefore these two tensors are attributed to a later transtensional tectonic phase (**D4**, Fig. 15), during which the NNW–SSE, dextral strike-slip faulting was dominant.

Accordingly, the obtained three tensors are related to two successive extensional phases, postdating sedimentation. They are labeled **D3** and **D4** as they logically follow the earlier extensional phase **D2** and the late Early Cretaceous compressional **D1a** and **D1b** (Fig. 15) which are discussed below.

The stress *Tensors 4*, *5* and *6* were calculated from faults in the basement rocks only (Figs. 4,9–11,13 and 14) and could not explain faults in the Paleogene sediments when imposed to them in controlling calculations. Therefore, they are considered older than the sediments. The *Tensors 4* and *5 were* obtained only from fault-slip data in Triassic limestones of the Struma unit, near Vaksevo (Fig. 13) and in the Poletintsi area (Fig. 9), below the major thrust contact (Kounov et al., 2010). This compression was related to the late Early Cretaceous emplacement of the Morava nappe on the Struma unit (Fig. 15), whereby the latter was deformed under brittle conditions (e.g. Zagorchev and Ruseva, 1982; Kounov et al.,

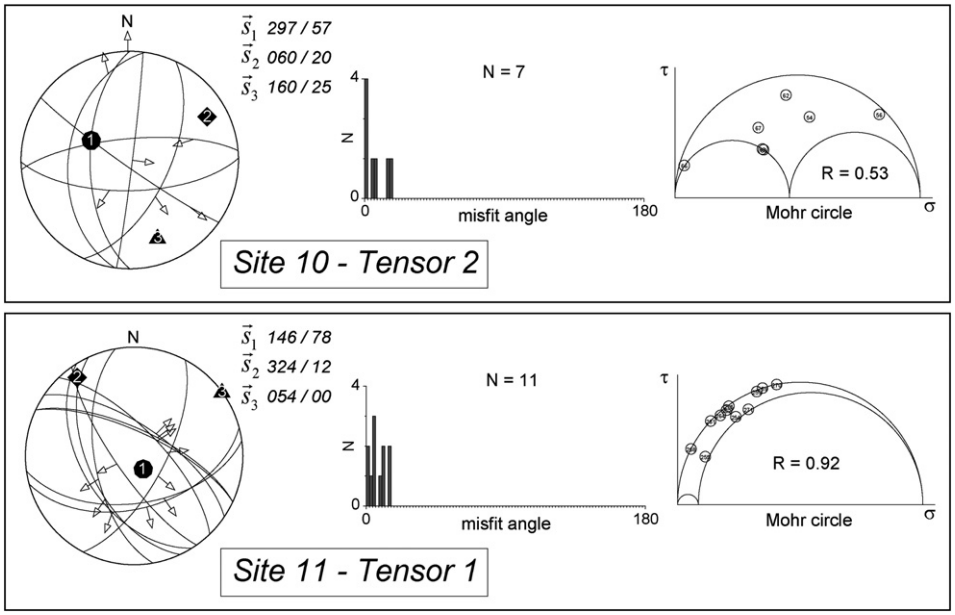

Fig. 14. Lower hemisphere, equal-area plots of brittle fault-slip striations from the Osogovo-Lisets metamorphics (*Site 11*) and Triassic limestones in Osogovo Mountain (*Site 10*). Localities of the sites are shown on Fig. 4. Legend as in Fig. 6.

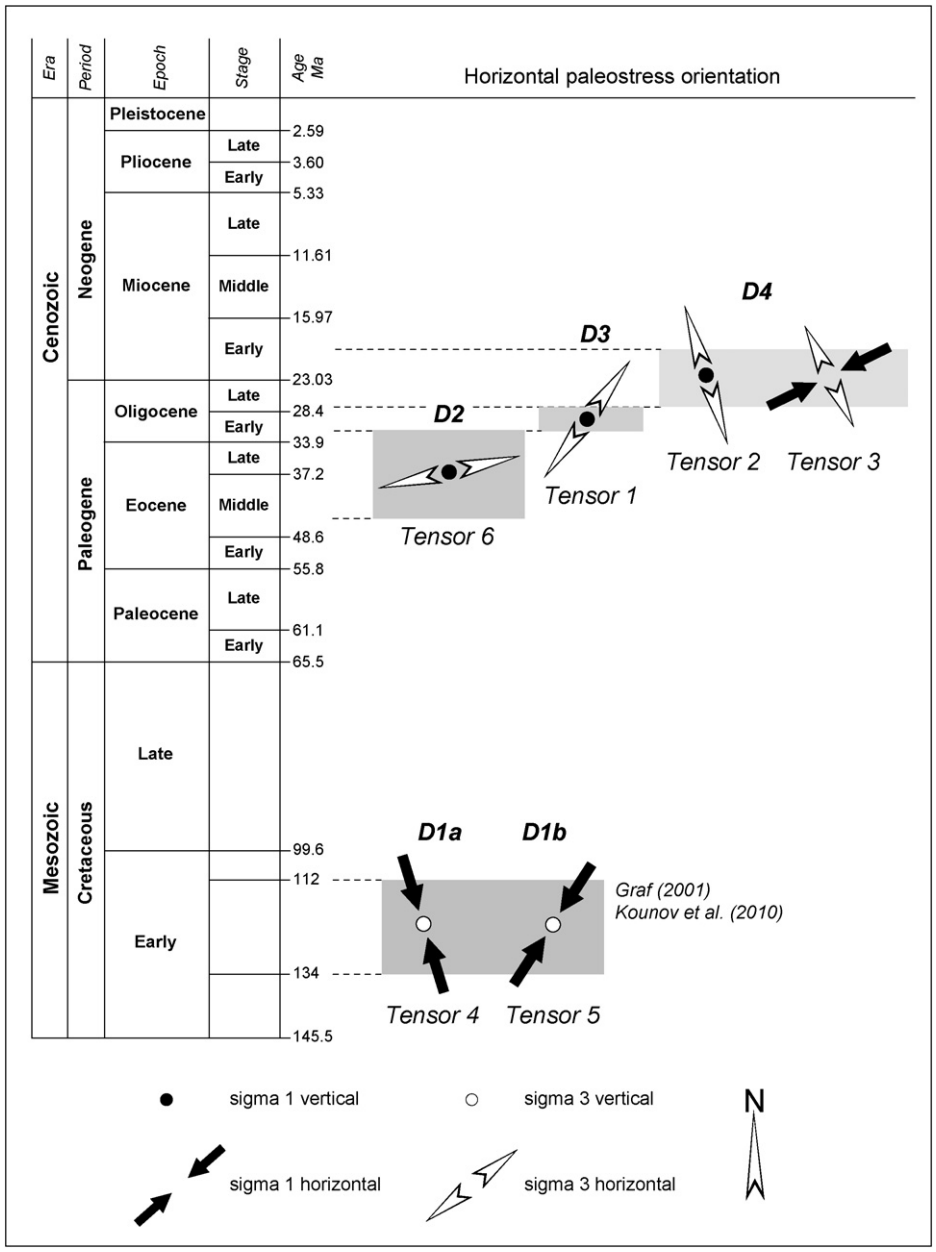

Fig. 15. Proposed time sequence and orientation of regional stress tensors. The numerical time scale from Gradstein et al. (2004).

2010). During this event, its structurally deeper parts – the Osogovo-Lisets Complex – underwent syn-metamorphic, ductile deformation (Kounov et al., 2010). The compressional pre-Cenozoic tectonics was out of the scope of this study and the two compressive tensors reported here were already discussed in Kounov et al. (2010). Tensors with similar orientation were obtained by Graf (2001) from the same area. Our data are insufficient for general conclusions but the *Tensor 1* fits the D1 deformation stage (**D1a** here) of Graf (2001) whereas the *Tensor 2* matches his D2 stage (phase **D1b** here). Both stages are reported as related to the late Early Cretaceous compression in the Kraishte zone Graf (2001).

The next major tectonic event was the middle Eocene–early Oligocene extension and the formation of sedimentary basins above major detachments (Kounov et al., 2004). The stress tensors obtained from measurements along the Dragovishtitsa detachment surface and minor fault planes in the area of Dragovishtitsa and Poletintsi (*Tensor 6*, Figs. 9–11) show WSW–ENE extension (**D2**, Fig. 15). Field relationships show that SW-dipping normal faults cut the reverse faults (Fig. 7c), which demonstrates that this tensor is younger than the previous ones (*Tensors 4* and *5*).

The **D2** tectonic phase is represented by the NW–SE to NNW–SSW normal faults in the hanging wall of the detachment system. The formation of the Pianets and Poletintsi basins was controlled by faulting at their SW border (Figs. 1 and 5), whereas the Prekolnitsa, Delchevo and Padesh basins had faulted margins in the northeast (Fig. 2). This phase corresponds to the syn-sedimentary tectonic stage of Moskovski and Harkovska (1973) with a major extensional axis trending between N050° and N070°. This extension was also contemporaneous with the ENE–WSW extension and formation of the Mesta Basin (Burchfiel et al., 2003), the deposition of thick volcano-sedimentary deposits, the formation of extensional core complexes in the Rhodope (e.g. Cernjavska, 1977; Boyanov and Goranov, 2001; Bonev et al., 2006; Brun and Sokoutis, 2007) and the formation of several basins in eastern Macedonia (i.e.

Ovchepole and Tikves basins, Dumurdzanov et al., 2005; Burchfiel et al., 2008). During the Eocene–Oligocene, the Kraishte zone was part of the so-called South Balkan extensional region (Burchfiel et al., 2000, 2003, 2008; Dumurdzanov et al., 2005; Schefer et al., 2010) formed during rollback of the Aegean slab (Jolivet et al., 2003; Jolivet and Brun, 2010).

By the end of the Eocene, the detachments were exposed and became inactive. This was the time of a marine transgression, which was accompanied in the early Oligocene by volcanic activity (Harkovska et al., 1989; Kounov et al., 2004). Sedimentation in basins continued until 32–29 Ma when the sediments were intruded by subvolcanic bodies and dykes often along the NW–SE fault structures (Harkovska and Pecskay, 1997; Kounov et al., 2004). The **D3** SW–NE extension probably corresponds to this stage also reported as post-sedimentary syn-magmatic phase by Moskovski (1971a).

Sedimentation continued with some interruptions into the late Oligocene, but without angular unconformity, accumulating continental coal-bearing deposits. Moskovski (1971a) relates the formation of the late Oligocene–earliest Miocene continental basins in Kraishte (Fig. 2, Sekirna, Bobov Dol and Pernik basins) to dextral strike-slip tectonics. This would correspond to the **D4** SSE–NNW transtension. The related strike-slip faults represent a possible continuation, in Bulgaria, of the Timok fault (Fig. 1), a major dextral strike-slip zone active during the Oligocene–early Miocene and responsible for up to 100 km displacement of the Cretaceous nappe edifice in the south Carpathians (e.g. Schmid et al., 2008). Faulting and basin formation in the Kraishte may have occurred in releasing bend zones along or at the termination of this fault zone. This would also explain the permutation of the $\vec{s}_1$ and $\vec{s}_2$ stress axes (between *Tensor 2* and *Tensor 3*, Fig. 15) whereby $\vec{s}_1$ is vertical within extensional, releasing bends and horizontal along the major strike-slip fault and restraining bends.

It is not clear yet what caused the almost 50° anticlockwise rotation of the extensional $\vec{s}_3$ axis between **D3** and **D4** (Fig. 15). The change in extension direction from NE–SW to N–S has taken place in the Aegean region only since the beginning of the Pliocene (~6 Ma) when the North Anatolian Fault extended into the northern Aegean Sea (Armijo et al., 1999). On the other hand, farther north in Serbia and Romania, northeastward lateral extrusion and rotation of continental fragments around the western boundary of Moesia induced generally N–S oriented orogen-parallel stretching (Boccaletti et al., 1974; Tapponnier, 1977; Burchfiel, 1980; Schmid et al., 1998; Fügenschuh and Schmid, 2005). This extrusion was accommodated by dextral strike-slip movements along the Cerna-Jiu and Timok fault zones (Fig. 1) from the late Eocene to the early Miocene (Burdigalian) (~20 Ma; e.g. Schmid et al., 1998; Fügenschuh and Schmid, 2005). Therefore one might suggest that since the late Oligocene extension in the Kraishte area was related to the crustal stretching associated with extrusion of continental fragments around the Moesian platform rather than to processes in the Aegean region. N–S extension in Bulgaria was also reported for the late Miocene, and probably even earlier, where it was related to the formation of the so-called Sub-Balkan E–W trending graben system (north of the Balkan chain, Fig. 1) and the Thrace basin (Tzankov et al., 1996; Nakov et al., 2001). Recently, Vangelov et al. (in press) have shown that most of the Sub-Balkan basins are pull-aparts formed during transtension.

Several authors attributed the early Miocene break in sedimentation in the southern Balkan Peninsula to a compressional phase (Nakov et al., 2001; Boyanov and Goranov, 2001; Dumurdzanov et al., 2004). Zagorchev (1993) reported folds and reverse faults in the Bobov Dol and Pernik basins. We have not been able to find such structures in the Paleogene basins studied here and suggest that they therefore do not have a regional expression. The local reverse faults and folds in question may have developed in restraining bend zones along the Timok strike-slip fault zone still active at that time, as is suggested for the northern border of the Pernik basin (Fig. 2, Gerdjikov and Georgiev, 2006).

The middle Miocene to Quaternary extension in the Kraishte area probably activated faults with a relatively small displacement bounding small basins filled with alluvial to lacustrine deposits. The center of extension and basin formation had shifted farther south to southern Bulgaria, Macedonia and northern Greece (Burchfiel et al., 2008).

6. Conclusions

The paleostress analysis on the fault data in Paleogene sediments and in the underlying basement allows the determination of successive faulting events during the Cenozoic tectonics of the Kraishte area.

Middle Eocene–early Oligocene brittle deformation in the hanging wall of active detachment systems was related to WSW–ENE extension. This extension led to the formation of half grabens filled with thick continental to marine deposits.

Between 32 and 29 Ma, the sediments and their basement were intruded by subvolcanic bodies and dykes probably under SW–NE extension. This tectonic event, together with the previous, similarly oriented extensional phase was probably part of the early stages of Aegean extension.

From the late Oligocene to the earliest Miocene, SSE–NNW transtension led to the formation of continental basins. The almost 50° anticlockwise rotation of the $\vec{s}_3$ axis from the previous tectonic stage was possibly related to a switch from slab-rollback-generated Aegean extension to crustal stretching associated with the extrusion of continental fragments around the Moesian platform.

Since the middle Miocene extension controlled the formation of small sedimentary basins along faults with a relatively small displacement.

Acknowledgments

This study was supported by the ETH Zurich, project No. 0-20657-99. We thank the entire Structural Geology and Tectonic research group from Sofia University, Bulgaria. We would like to thanks also Bernard Célérier from University of Montpellier for introducing AK to his paleostress analysis software. The reviews of two anonymous reviewers helped to clarify the original manuscript.

Appendix. Supplementary material

Supplementary data related to this article can be found online at doi:10.1016/j.jsg.2011.03.006.

References

Anderson, E.M., 1951. The Dynamics of Faulting and Dyke Formation with Applications to Britain. Oliver & Boyd, Edinburgh, p. 191.
Angelier, J., 1979. Determination of the mean principal direction of stresses for a given fault population. Tectonophysics 56, 17–26.
Angelier, J., Tarantola, A., Valette, B., Manoussis, S., 1982. Inversion of field data in fault tectonics to obtain the regional stress; I, single phase fault populations: a new method of computing the stress tensor. Geophysical Journal of the Royal Astronomical Society 69, 607–621.
Armijo, R., Meyer, B., Hubert, A., Barka, A., 1999. Westward propagation of the North Anatolian fault into the northern Aegean: timing and kinematics. Geology 27, 267–270.
Bakalov, P., Jelev, V., 1996. Lithostratigraphy of the Neogene–Villafrancian sediments of the Kjustendil graben. Review of the Bulgarian Geological Society 57, 75–82 (in Bulgarian, with English abstract).
Boccaletti, M., Manetti, P., Peccerillo, A., 1974. Hypothesis on the plate tectonic evolution of the Carpatho-Balkan Arcs. Earth Planetary Science Letters 23, 193–198.

Belmoustakov, E., 1948. La géologie de la partie méridionale de la région Pianec (Bulgarie). Revue de la Société Géologique Bulgare 20, 1–63 (in Bulgarian, with French abstract).
Bonchev, E., 1936. Versuch einer tektonischen Synthese Westbulgariens. Geologica Balcanica 2, 5–48.
Bonchev, E., 1971. Problems of the Bulgarian Geotectonics. Technica, Sofia, p. 204.
Bonchev, E., Karagiuleva, J., Kostadinov, V., Manolov, Z., Kamenova, J., Dinkov, E., Bakalova, D., Manolova, R., 1960. Grundlagen der Tektonik von Kraiste mit den angrenzenden Gebieten. Travaux sur la Géologie Bulgare. Série Stratigraphie et Tectonique 1, 7–92 (in Bulgarian, with German abstract).
Bonev, N., Burg, J.-P., Ivanov, Z., 2006. Mesozoic–Tertiary structural evolution of an extensional gneiss dome – the Kesebir-Kardamos dome, eastern Rhodope (Bulgaria–Greece). International Journal of Earth Sciences 95, 318–340.
Bott, M.H.P., 1959. The mechanics of oblique slip faulting. Geological Magazine 96, 109–117.
Boyanov, I., Goranov, A., 2001. Late Alpine (Palaeogene) superimposed depressions in parts of Southeast Bulgaria. Geologica Balcanica 31, 3–36.
Brun, J.-P., Sokoutis, D., 2007. Kinematics of the southern Rhodope core complex (North Greece). International Journal of Earth Sciences 96, 1079–1099.
Burchfiel, B.C., 1980. Eastern European Alpine system and the Carpathian Orocline as an example of collision tectonics. Tectonophysics 63, 31–61.
Burchfiel, B.C., Nakov, R., Tzankov, T., Royden, L., 2000. Cenozoic extension in Bulgaria and northern Greece: the northern part of the Aegean extensional regime. In: Bozkurt, E., Winchester, E., Piper, J.D.A. (Eds.), Tectonics and Magmatism in Turkey and the Surrounding Area. Geological Society, London, Special Publications, vol. 173, pp. 325–352.
Burchfiel, B.C., Nakov, R., Tzankov, T., 2003. Evidence from the Mesta half graben, SW Bulgaria, for the late Eocene beginning of Aegean extension in the central Balkan Peninsula. Tectonophysics 375, 61–76.
Burchfiel, B.C., Nakov, R., Domurdzanov, N., Papanikolau, D., Tzankov, T., Serafimovski, T., King, R.W., Kotzev, V., Todosov, A., Nurce, B., 2008. Evolution and dynamics of the Cenozoic tectonics of South Balkan extensional system. Geosphere 4, 919–938.
Célérier, B., 1988. How much does slip on reactivated fault plane constrain the stress tensor? Tectonics 7, 1257–1278.
Célérier, B., 1995. Tectonic regime and slip orientation of reactivated faults. Geophysical Journal 121, 143–161.
Célérier, B., 1999. Fault Slip Analysis Software. http://www.pages-perso-bernard-celerier.univ-montp2.fr/software/dcmt/fsa/fsa.html.
Cernjavska, S., 1977. Palynological studies on Paleogene deposits in South Bulgaria. Geologica Balcanica 7, 3–26.
Compton, R.R., 1966. Analyses of Pliocene–Pleistocene deformation and stresses in northern Santa Lucia Range, California. Geological Society of America Bulletin 77, 1361–1379.
Dimitrov, C., 1931. Contribution to the geology and petrography of the Konyavo mountain. Review of the Bulgarian Geological Society 3, 3–52 (in Bulgarian).
Dumurdzanov, N., Serafimovski, T., Burchfiel, B.C., 2004. Evolution of the Neogene–Pleistocene Basins of Macedonia. In: Geological Society of America Digital Map and Chart Series 1 (Accompanying Notes). Boulder, Colorado, 20 pp.
Dumurdzanov, N., Serafimovski, T., Burchfiel, B.C., 2005. Cenozoic tectonics of Macedonia and its relation to the South Balkan extensional regime. Geosphere 1, 1–22.
Etchecopar, A., Vassuer, G., Daignieres, M., 1981. An inverse problem in microtectonics for the determination of stress tensors from fault striations analysis. Journal of Structural Geology 3, 51–65.
Fügenschuh, B., Schmid, S.M., 2005. Age and significance of core complex formation in a very curved orogen: evidence from fission track studies in the South Carpathians (Romania). Tectonophysics 404, 33–53.
Gautier, P., Brun, J.P., Moriceau, R., Sokoutis, D., Martinod, J., Jolivet, L., 1999. Timing, kinematics and cause of Aegean extension: a scenario based on a comparison with simple analogue experiments. Tectonophysics 315, 31–72.
Gerdjikov, I., Georgiev, N., 2006. The Maritsa fault system – a strike-slip zone along the northern margin of the Rhodopes. Annual of the University of Mining and Geology "St. Ivan Rilski" 49, 33–39.
Gradstein, F., Ogg, J., Smith, A., 2004. A Geologic Time Scale 2004. Cambridge University Press, Cambridge, 589 pp.
Graf, J., 2001. Alpine tectonics in Western Bulgaria: Cretaceous compression of the Kraishte region and Cenozoic exhumation of the crystalline Osogovo-Lisets Complex, PhD thesis. ETH, Zürich.
Hancock, P.L., 1985. Brittle microtectonics: principles and practice. Journal of Structural Geology 7, 437–457.
Harkovska, A., 1974. Structure of the Prekolnitsa graben (SW Bulgaria). Review of the Bulgarian Geological Society 35, 239–251 (in Bulgarian, with English abstract).
Harkovska, A., Pecskay, Z., 1997. The Tertiary magmatism in Ruen magmato-tectonic zone (W. Bulgaria) – a comparison of new K-Ar ages and geological data. In: Boev, B., Serafimovski, T. (Eds.), Magmatism, Metamorphism and Metallogeny of the Vardar Zone and Serbo-Macedonian Massif. Faculty of Mining Geology, Stip-Dojran, Republic of Macedonia, pp. 137–142.
Harkovska, A., Yanev, Y., Marchev, P., 1989. General features of the Paleogene orogenic magmatism in Bulgaria. Geologica Balcanica 19, 37–72.
Heuberger, S., Célérier, B., Burg, J.P., Chaudhry, N.M., Dawood, H., Hussein, S., 2010. Paleostress regimes from brittle structures of the Karakoram-Kohistan Suture Zone and surrounding areas of NW Pakistan. Journal of Asian Earth Sciences 38, 307–335. doi:10.1016/j.jseaes.2010.01.004.
Jolivet, L., Brun, J.-P., 2010. Cenozoic geodynamic evolution of the Aegean. International Journal of Earth Sciences 99, 109–138.
Jolivet, L., Daniel, J.M., Truffert, C., Goffé, B., 1994. Exhumation of deep crustal metamorphic rocks and crustal extension in arc and back-arc regions. Lithos 33, 3–30.
Jolivet, L., Facenna, C., Goffé, B., Burov, E., Agard, P., 2003. Subduction tectonics and exhumation of high-pressure metamorphic rocks in the Mediterranean orogens. American Journal of Science 303, 353–409.
Kamenov, B., 1942. Über die Geologie des nordwestlichen Teils des Kustendilgebiets. Jahrbuch der Direktion für Bodenschätze in Bulgarien (A)2, pp. 1–35. (in Bulgarian, with German abstract).
Kounov, A., 2002. Thermotectonic evolution of Kraishte zone, Western Bulgaria, PhD thesis. ETH, Zürich.
Kounov, A., Seward, D., Bernoulli, D., Burg, J.-P., Ivanov, Z., 2004. Thermotectonic evolution of an extensional dome: the Cenozoic Osogovo-Lisets core complex (Kraishte zone, western Bulgaria). International Journal of Earth Sciences 93, 1008–1024.
Kounov, A., Seward, D., Burg, J.-P., Bernoulli, D., Ivanov, Z., Handler, R., 2010. Geochronological and structural constraints on the Cretaceous thermotectonic evolution of the Kraishte zone (Western Bulgaria). Tectonics 29, TC2002. doi:10.1029/2009TC002509.
Moskovski, S., 1968a. On the Fault-fold Paragenesis of Some Paleogenic Grabens in the Kraishtid Structural Zone. In: Geological Institute of BAN and the Committee of Geology, Jubilee Geological Volume, pp. 147–155. (in Bulgarian, with English abstract.
Moskovski, S., 1968b. Tectonic of the Pianec grabens complex south of Kjustendil. Structural stages. Bulletin of the Geological Institute, Series Geotectonics, Stratigraphy and Lithology 17, 143–158 (in Russian).
Moskovski, S., 1969. Tektonik eines Teiles des Pijanec-Grabenkomplexes südlich von Kjustendil Störungen. In: Annual of the Sofia University, Faculty of Geology and Geography, vol. 1, pp. 141–156. (in Bulgarian, with German abstract).
Moskovski, S., 1971a. On the sequence in the formation of Paleogene–Neogene graben structures in the Kraishtides in Bulgaria. Review of the Bulgarian Geological Society 32, 21–31 (in Bulgarian, with English abstract).
Moskovski, S., 1971b. On the Structure of the Poletintsi Paleogene Graben. In: Annual of the Sofia University, Faculty of Geology and Geography, vol. 2, pp. 77–87. (in Bulgarian, with English abstract).
Moskovski, S., Harkovska, A., 1973. Main stages in the Late Alpine development of some fault zones in a part of South-Western Bulgaria. In: Annual of the Sofia University, Faculty of Geology and Geography, vol. 1, pp. 73–84. (in Bulgarian, with English abstract).
Moskovski, S., Shopov, V., 1965. Stratigraphy of the Paleogene and the resedimentation phenomena (olistostromes) related to it in Pyanets area, Kjustendil district (SW Bulgaria). Bulletin of the Institute of Geology, Stratigraphy and Lithology 16, 189–209 (in Bulgarian, with English abstract).
Nakov, R., Burchfiel, B.C., Tzankov, T., Royden, L.H., 2001. Late Miocene to Recent Sedimentary Basins of Bulgaria. In: Geophysical Society of America Map and Chart Series, vol. 88, Scale 1:200,000, p. 28.
Petit, J.P., 1987. Criteria for the sense of movement on fault surfaces in brittle rocks. Journal of Structural Geology 9, 597–608.
Schefer, S., Cvetković, V., Fügenschuh, B., Kounov, A., Ovtcharova, M., Schaltegger, U., Schmid, S., 2010. Cenozoic granitoids in the Dinarides of southern Serbia: age of intrusion, isotope geochemistry, exhumation history and significance for the geodynamic evolution of the Balkan Peninsula. International Journal of Earth Sciences. doi:10.1007/s00531-010-0599-x.
Schmid, S.M., Berza, T., Diaconescu, V., Froitzheim, N., Fügenschuh, B., 1998. Orogen-parallel extension in the southern Carpathians. Tectonophysics 297, 209–228.
Schmid, S.M., Bernoulli, D., Fügenschuh, B., Matenco, S., Schefer, L., Schuster, R., Tischler, M., Ustaszewski, K., 2008. The Alps-Carpathians-Dinarides-connection: a compilation of tectonic units. Swiss Journal of Geosciences 101, 139–183.
Sippel, J., Scheck-Wenderoth, M., Reicherter, K., Mazur, S., 2009. Paleostress states at the southwestern margin of the central European Basin system-application of fault-slip analysis to unravel a polyphase deformation pattern. Tectonophysics 470, 129–146. doi:10.1016/j.tecto.2008.04.010.
Sperner, B., Ratschbacher, L., Ott, R., 1993. Fault-striae analysis: a Turbo Pascal program package for graphical presentation and reduced stress tensor calculation. Computers and Geosciences 19, 1361–1388.
Tapponnier, P., 1977. Evolution tectonique du système alpin en Méditerranée: poinçonnement et écrasement rigide-plastique. Bulletin de la Société géologique de France 7, 437–460.
Tzankov, T., Angelova, D., Nakov, R., Burchfiel, B.C., Royden, L.H., 1996. The Sub-Balkan graben system of central Bulgaria. Basin Research 8, 125–142.
Vangelov, D., Gerdjikov, I., Bonev, K., Dimitrov, S., in press. Preliminary data of the Karlovo Basin formation and evolution. Annuaire de l'Université de Sofia, Faculté de Géologie et Géographie. (in Bulgarian, with English abstract).
Vardev, N., 1987. Structure of the Ruen ore district. PhD thesis, Sofia University.
Viola, G., Venvik Ganerød, G., Wahlgren, C.-H., 2009. Unravelling 1.5 Gyr of brittle deformation history in the Laxemar-Simpevarp area, SE Sweden: a contribution to the Swedish site investigation study for the disposal of highly radioactive nuclear waste. Tectonics 28, TC5007. doi:10.1029/2009TC002461.
Yamaji, A., 2000. The multiple inverse method: a new technique to separate stresses from heterogeneous fault-slip data. Journal of Structural Geology 22, 441–452. doi:10.1016/S0191-8141(99)00163-7.
Zagorchev, I., 1993. Radomir and Bosilegrad Map Sheets with Explanatory Notes. Geological Map of Bulgaria on scale 1:100 000, Sofia.

Zagorchev, I., 2001. Introduction to the geology of SW Bulgaria. Geologica Balcanica 31, 3–52. Special issue "Geodynamic Hazards (Earthquakes, Landslides), Late Alpine Tectonics and Neotectonics in the Rhodope Region".
Zagorchev, I., Popov, N., 1968. Geology of Padesh Paleogene basin. In: Geological Institute of BAN and Committee of Geology, Jubilee Geological Volume pp. 23–35. (in Bulgarian, with English abstract).
Zagorchev, I., Ruseva, M., 1982. Nappe structure of the southern parts of Osogovo. Geologica Balcanica 12, 35–57 (in Russian, with English abstract).
Zagorchev, I., Ruseva, M., 1993. Kriva Palanka and Kjustendil Map Sheets with Explanatory Notes. Geological Map of Bulgaria on scale 1:100 000, Sofia.
Zagorchev, I., Popov, P., Ruseva, M., 1989. Paleogene stratigraphy in a part of SW Bulgaria. Geologica Balcanica 19, 41–69 (in Russian, with English abstract).